Microporous and Mesoporous Materials 153 (2012) 191–197

Contents lists available at SciVerse ScienceDirect

Microporous and Mesoporous Materials

journal homepage: www.elsevier.com/locate/micromeso

Synthesis and characterization of a novel composite: Polyindole included in nanostructured Al-MCM-41 material

Marcos B. Gómez Costa, Juliana M. Juárez, María L. Martínez, Jorgelina Cussa, Oscar A. Anunziata *

Centro de Investigación en Nanociencia y Nanotecnología (NANOTEC), Facultad Regional Córdoba, Universidad Tecnológica Nacional, Maestro López y Cruz Roja Argentina, 5016 Córdoba, Argentina

ARTICLE INFO

Article history:
Received 14 October 2011
Received in revised form 20 December 2011
Accepted 21 December 2011
Available online 28 December 2011

Keywords:
Composite
PInd–Na-AlMCM-41
Polyindole
Molecular nanowire
Na-AlMCM-41

ABSTRACT

Polyindole/MCM-41 composite material was prepared from a mesoporous aluminosilicate, Na-AlMCM-41 used as host, by an oxidative in situ polymerization of pre-adsorbed indole, employing Cl_3Fe as oxidant. Studies of infrared spectroscopy and UV–Vis spectroscopy indicate that it was possible to obtain in situ polymerization of indole (PInd molecular wire), creating a new nano-composite PInd–Na-AlMCM-41 with conductive properties and a potential material for electro-catalytic processes. The thermal properties of polyindole, Na-AlMCM-41, and the composite obtained were also investigated by TGA analyses indicating that the polymer has a higher thermal stability when forming nanowires in the composite. Conductivity studies show that PInd–Na-AlMCM-41 exhibits semiconductor behavior at room temperature and its conductivity was in the range of 4×10^{-3} S cm^{-1}.

1. Introduction

Na-Al-MCM-41 belongs to M41S, the collective name for a family of crystalline mesoporous molecular sieves with a regular and well-defined mesoporous system. Na-Al-MCM-41 shows uniform channels and their pore diameter can be varied systematically between 1.5 and 10 nm through the choice of surfactant as the template, auxiliary chemicals and reaction conditions. Due to its regular pore structure and pore shape, MCM-41 has been considerably studied as a model substance for sorption of various gases and vapors [1]. Other interesting physical properties include highly specific surface up to 1000 m^2/g, specific pore volume up to 1.3 mL/g, and high thermal stability; all of these allowing for many applications. Processing information at the molecular level is an intriguing and key challenge. Efforts to create electronic functions and devices based on molecules instead of bulk semiconductors are inspired by the anticipated major increase in computing speed and storage density. Mesoporous molecular sieves of type MCM-41, with a hexagonal packed array of channels and a narrow pore size distribution offer unique opportunities for the preparation of new nanostructured composite materials [2,3].

The study of the electroactive properties of heterocyclic conducting polymers containing nitrogen atoms like polyaniline, polypyrrole, polycarbazole and their substituted derivatives [1,2] has attracted considerable interest due to their potential industrial applications.

Among these polymers, polypyrrole displays high electrical conductivity, good environmental stability and fine for anodic electrodeposition of freestanding polypyrrole films. On the other hand, poly(para-phenylene) exhibits good thermal stability. Indole has benzene and pyrrole ring. Thus, polyindole and its derivatives may possess the properties of poly(paraphenylene) and polypyrrole in concert. However, among various aromatic-compound-based conducting polymers, polyindole and its derivatives have been investigated only scarcely, although close structural similarities can be found with the polymers mentioned above [4].

Polyindole is an electroactive polymer which can be obtained either anodic or by chemical oxidation of indole, C_8NH_7. Polyindole films exhibit fairly good thermal stability, high-redox activity and stability, and slow degradation rate compared with polyaniline and polypyrrole.

This polymer and its derivatives seem to be good candidates for applications in domains including electronics, electrocatalysis and pharmacology. In its doped state, polyindole is green, with an electrical conductivity in the range of 5×10^{-4}–8×10^{-2} S cm^{-1}, slightly depending on the nature of the counter-ion [5]. It has also been reported that polyindole films have show fairly good thermal stability, high redox activity and slow degradation rate in comparison with polypyrrole and polyaniline [6].

There are many published works studying the electrochemical properties of polyindole for use in battery electrodes [4,7,8]. Nanocomposites of polyindole (PInd) and ZnO were prepared by

* Corresponding author. Tel./fax: +54 351 4690585.
E-mail address: oanunziata@scdt.frc.utn.edu.ar (O.A. Anunziata).

1387-1811/$ - see front matter © 2011 Elsevier Inc. All rights reserved.
doi:10.1016/j.micromeso.2011.12.044

chemical polymerization by Mispa et al. [9] to be used in corrosion protection and as a nano light-emitting device in electronics. Joshi and Prakash 10] recently published a composite of nanosized gold and polyindole that it was prepared via in situ polymerization of indole in a one-pot synthesis and determined its nanoscale electrical properties.

In this work we study indole adsorption on a mesoporous aluminosilicate (Na-AlMCM-41) and the in situ polymerization that confers unique properties to the composite. These results were not reported in the literature, and no development of indole polymerization into this host could be found. This work constitutes a valuable contribution to the field of nanostructured materials.

This work aims at synthesizing PInd–Na-AlMCM-41 composites, using in situ polymerization techniques, in order to obtain a new nanocomposite with conductive properties and potential catalysts for electrocatalytic processes.

2. Experimental

2.1. Materials

Tetraethylorthosilicate (TEOS, 98%, Sigma–Aldrich), cetyltrimethylammonium bromide (CTAB, Sigma–Aldrich), sodium-aluminate ($NaAlO_2$, Riedel-de Haän), ammonium hydroxide (25% wt Sigma–Aldrich), ferric chloride (Sigma–Aldrich), indole (Acros Organics).

2.2. Synthesis of Si-MCM-41 and Na-Al-MCM-41

The Si and Al-containing-MCM-41 nanostructured material was synthesized to be applied in the preparation of composites. In this study, the material used as hosts, was obtained employing the sol–gel method.

The mesoporous silicate was synthesized by hydrolysis of tetraethylorthosilicate (TEOS) at room temperature, in an aqueous solution, using cetyltrimethylammonium bromide (CTAB) as a surfactant. The procedure designed is described as follows: the surfactant was dissolved in de-ionized water and stirred until the solution was homogeneous and clear. After adding an adequate volume of ammonium hydroxide (25% w/w), the mixture was stirred for 5 min after which TEOS was added. The molar composition of the gel was 1 M TEOS:1.64 M NH_4OH:0.15 M CTAB:126 M H_2O. The reaction was stirred overnight after which the solution was filtered and washed consecutively with de-ionized water, and dried at room temperature [11].

To remove the template, the sample was heated up from ambient temperature to 723 K under N_2 flow (20 mL/min) and subsequently calcined, under air flow (10 mL/min), up to 723 K using a heating rate of 3 K/min [12].

The alumination procedure of MCM-41 was carried out as follows [13,14]: silica MCM-41 (1 g) was stirred for 20 h at room temperature in 50 mL of water containing dissolved sodium-aluminate. The mixture was filtered, washed, dried at room temperature overnight and then calcined in air at 823 K for 5 h. Finally, Na-AlMCM-41 sample with Si/Al = 20 was obtained, according to ICP analysis. The synthesis was effectively performed with the technique developed. The material characterization indicates the regularity of the hexagonal array of cylindrical pores in the Na-AlMCM-41.

2.3. Polyindole ex-situ preparation

Polyindole (PInd) was synthesized by chemical polymerization of indole monomer, C_8NH_7, using $FeCl_3$ as an oxidant. 0.35 g of indole was dissolved in deionized water at 338 K. This solution was kept at 338 K for 30 min stirring continuously. Afterwards, a solution of $FeCl_3$ 0.1 M was added. The reaction was left 24 h, filtered and washed with water and ethanol. The solid product was maintained at 313 K for 48 h, to obtain pure PInd.

2.4. Indole adsorption

Na-Al-MCM-41 sample, employed as a host, was dehydrated at 673 K in vacuum for 1 h. After it was exposed to equilibrium vapors from indole during 24 h at 333 K to obtain indole saturated hosts according to the procedure described by Anunziata et al. [15–17]. In these conditions, the indole/host saturation relation was reached. The color of the samples changed from white to beige (Ind–Al-MCM-41). For FTIR studies Self-supported Ind–Al-MCM-41 wafers in a vacuum cell with CaF_2 windows were used. The spectrum was first recorded in air and then in vacuum for 1 h at room temperature at 323, 373, 473, 573 and 673 K.

2.5. Indole in situ polymerization

The oxidative in situ polymerization to produce polyindole/Na-AlMCM-41 (PInd–Na-AlMCM-41) composite was performed similar to [15] using $FeCl_3$ as oxidant. The process was carried out adding 30 mL of $FeCl_3$ 0.1 M to the sample, in a beaker for 24 h, without stirring. Afterwards, the material was filtered and washed with ethanol and distilled water, and then dried at 333 K. This condition was kept for at least 72 h.

2.6. Characterization

The surface area was determined by the BET method with a Micromeritics Chemisorb 2720 apparatus, equipped with a TCD detector. A single-point surface area method was used and N_2 was employed as a physisorbed gas. The X-ray diffraction (XRD) patterns were recorded in a 2θ range from 1.6° to 8° (2θ) with a Philips X'Pert PRO PANalytical diffractometer under Cu Kα radiation (l = 0.154 nm). The diffraction data were collected using a continuous scan mode with a scan speed of 0.02 deg (2θ)/min. Thermal studies (TGA) of the guest, hosts and composites were carried out with a thermal analysis instrument (TA Instruments 2950 TGA-DSC). The samples were exposed to a constant heating rate of 10 K/min from room temperature to 873 K, under nitrogen flow (10 mL/min). FTIR studies were performed in a JASCO 5300 Fourier transform infrared spectrometer (FTIR). A vacuum heating cell with CaF_2 windows was used for measuring FTIR of self-supporting wafers of Ind–Al-MCM-41 and PInd–Na-AlMCM-41. Scanning electron micrographs (SEM) were obtained on a FE-SEM sigma. Direct current electrical conductivity measurements were performed using pellets improving the contacts with a silver layer.

3. Results and discussion

3.1. FTIR studies

Before the in situ polymerization, indole adsorption on Na-AlMCM-41 was characterized by thermo-infrared spectroscopy analysis.

Fig. 1a shows FTIR spectra in the region of 1300–1700 cm^{-1} for indole adsorbed on Na-AlMCM-41 and pure indole. When indole is adsorbed onto Na-AlMCM-41 material, Ind–AlMCM-41 shows bands at 1618, 1577, 1504, 1490, 1455, 1413, 1352 and 1334 cm^{-1} [18,19]. The bands at 1615 cm^{-1} overlap with the vibrations of water bending (a broad band at 1630 cm^{-1}) and Si–O stretching overtone of the AlMCM-41 framework vibration [17].

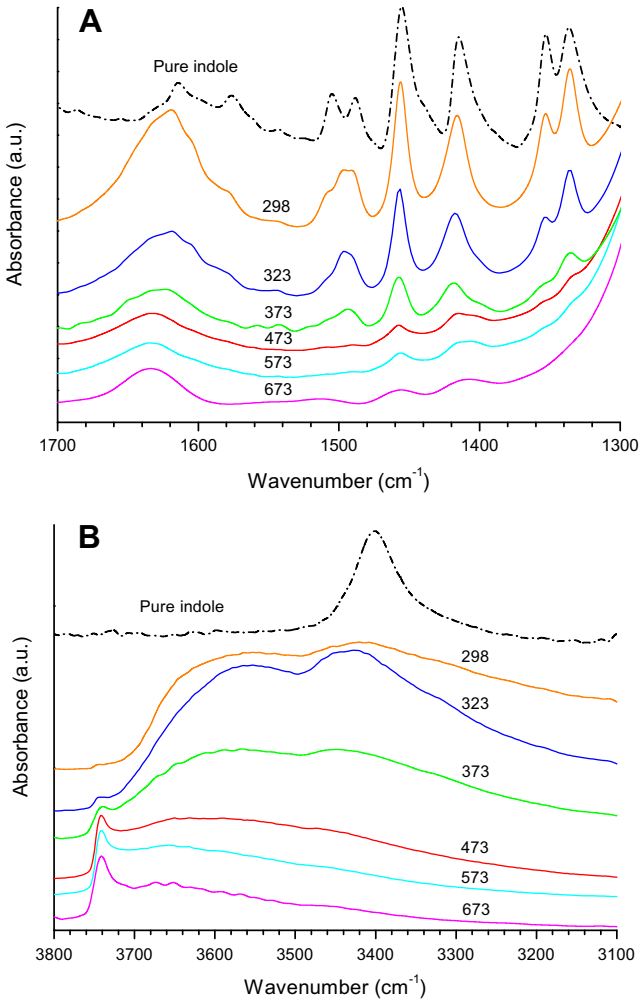

Fig. 1. FTIR of pure indole and indole adsorbed on Na-AlMCM-41 (Ind–AlMCM-41) treatment in vacuum at 298, 323, 373, 473, 573 and 673 K, in the range of (A) 1300–1700 cm^{-1} and (B) 3100–3800 cm^{-1}.

The bands do not shift from their locations in the spectrum of pure indole, indicating the weak interaction between indole and the AlMCM-41 mesostructure. On the other hand, the presence of an N–H group attached to a pyrrole ring and benzene ring in the indole increases the electron density of the pyrrole ring; this is due to the fact that there is an unshared electron pair on the NH group. Upon delocalization, this electron pair forms part of the π-system of the ring, with the consequent activation of all positions of the nucleus. Then, the sorption of the indole is expected to result mainly from the interaction of the π-electrons of the aromatic ring with electron-acceptor sites of the AlMCM-41, such as sodium cations or perhaps SiOH groups. As the sodium cations are strongly held to the Al-MCM-41 framework, due to the low capacity for electron delocalization of the MCM-41 structure, and taking into account that the structure of MCM-41 can be considered as a weak but hard base (as a function of molecular orbital theory) [16], π interactions of the aromatic base with structural SiOH groups of the Na-AlMCM-41 framework would be more probable. Then, indole would be held over the MCM-41 mesostructure only through such π interactions in the Ind–Al-MCM-41 sample. Table 1 shows the main bands.

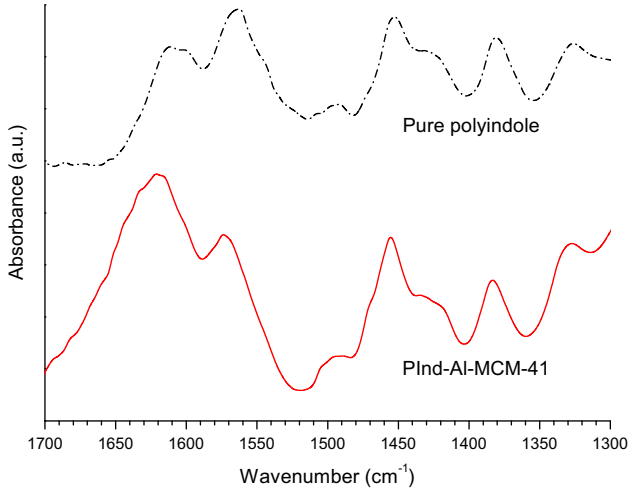

Fig. 2. FTIR of pure polyindole and PInd–Na-AlMCM-41 composite in the range of 1300–1700 cm^{-1}.

Fig. 1b exhibits infrared spectra in the region of 3100–3800 cm^{-1}. A band at 3742 cm^{-1} attributed to hydroxyl species due to silanol groups (Si–OH) [17] not appearing at room temperature became sharp when the sample is heated at 673 K. A broad indole band corresponding to N–H stretching is observed at 3415 cm^{-1}.

Fig. 2 shows FTIR spectra of polymer and composite (PInd–Na-AlMCM-41). The bands assigned are shown in Table 1. The FTIR absorption bands of pure PInd allowed us to identify some specific PInd–Na-AlMCM-41 bands (see Table 1).

Table 1
IR-band assignments of pure indole and polyindole, indole adsorbed on Al-MCM-41 (Ind–Al-MCM-41) and PInd–Na-AlMCM-41 composite.

Assignment	Band position, wavenumber (cm^{-1})*			
	Indole	Ind–Al-MCM-41	Polyindole	PInd–Na-AlMCM-41 composite
νNH	3415	3400	–	–
H_2O bending	1630	1630	–	1630
$\nu C_7C_8 + \nu C_5C_6 + \nu C_8C_9$	1614	1618	1612	1615
$\nu C_9C_4 + \nu C_6C_7 + \nu C_7C_8$	1577	1578	–	–
N-H Vibration	–	–	1564	1574
$\nu N_1C_2 + \delta C_2H$	1504	1508	1508	1505
$\nu C_8C_9 + \delta C_4H + \delta C_7H$	1490	1493	1493	1495
$\delta C_5H + \nu C_8N + \nu C_4C_5$	1455	1455	1452	1454
Stretch of C–N bond	–	–	1427	1429
$\delta NH + \nu C_2C_3 + \delta C_6H$	1413	1415	–	–
Stretching aromatic ring	–	–	1380	1383
$\nu C_8N + \delta C_6H + \nu C_2C_3$	1352	1354	–	–
Stretching of pyrrole ring	1336	1336	1326	1327

* [4,18,19].

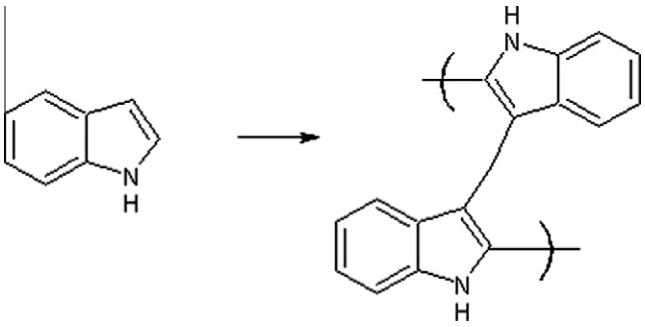

Fig. 3. Polymerization reaction of polyindole.

Bands can be observed at 1630, 1615, 1574, 1510, 1490, 1454, 1383 and 1325 cm^{-1} identified according to previous works (Table 1) [4,18,19].

There are two main opinions on the polymerization mechanism of indole, 1,3 position or 2,3 position (Figs. 3 and 4) [18]. The benzene ring is not usually involved in the polymerization process. The band at 1564 cm^{-1} could be assigned to N–H bond vibrations in the pure polymer [19] and this band shifts to a higher wavenumber in the composite. These results imply that there are still N–H bonds in the polymer backbone and in PInd–Na-AlMCM-41; however, it is more perturbed due to the polymer backbone.

Thus, nitrogen species may not be polymerization sites, and polymerization should mainly occur at the 2,3 position. The benzene ring is not affected in the polymerization process and 2,3 position of the pyrrole ring is responsible for the polymerization. In addition, bands at 1615, 1454 and 1380 cm^{-1} are induced by different stretchings of aromatic ring in the polymer chain [19]. The bands observed at 1427–1429 cm^{-1} are assigned to C–N stretching.

Some PInd bands shift with respect to pure PInd, due to the interaction of PInd with the host. Adsorbed water could be observed over the material at 1630 cm^{-1} overlapped with 1615 cm^{-1} band.

3.2. X-ray diffraction, SEM and BET studies

Fig. 5a displays the XRD analyses of Si-MCM-41. The XRD pattern for the as-synthesized sample exhibits a strong (100) reflection peak with two small peaks (second- and third-order peaks corresponding to (110) and (200) diffraction planes), characteristic of MCM-41 material. After the template was removed by calcination, the intensity of (100) diffraction was slightly increased, indicating that proper calcinations lead to a better-defined structure of MCM-41 [11,13,14,20].

Fig. 5b shows that diffraction patterns of aluminated sample suggest the preservation of the MCM-41 structure after incorporation of Al by post-synthesis method.

Only a slight broadening of the (100) reflection peaks for the Na-AlMCM-41 obtained by post-synthesis can be observed, as well as a slight shifting of the (100) peak to higher 2θ values and lower d-spacing after Al incorporation (Table 2). The same behavior has been reported for Al-SBA-3 obtained by grafting [13,14]. This behavior might be caused by a slight distortion of the mesoporous channels due to the partial polymerization over pore structures induced by superficial reaction. The sharpness of each of these XRD peaks indicates the regularity of the hexagonal array of pores in these substrates. The characteristic XRD d_{100} parameter is shown in Table 2.

Moreover, XRD patterns of the PInd–Na-AlMCM-41 composite (Fig. 5b) indicate that the hexagonal-ordered structure of MCM-41 was persistent, after the in situ polymerization procedure, seen in Table 2. In this figure it can be noted that plane (100) in the composite, characteristic of MCM-41, shifts to higher 2θ angles.

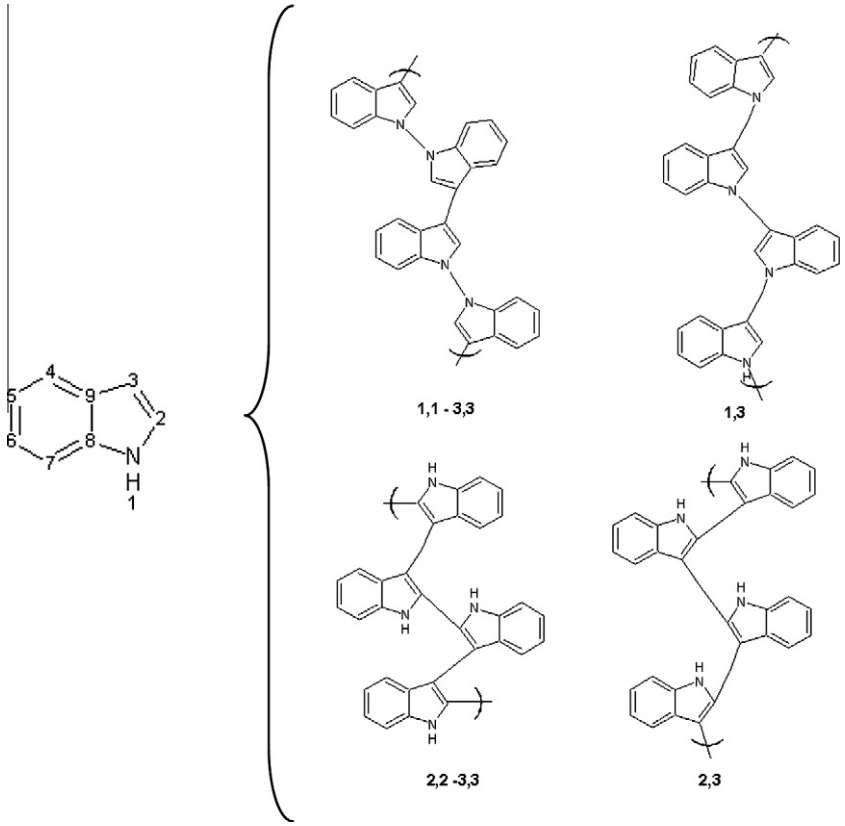

Fig. 4. Representation of indole monomer and the possible structures of polyindole.

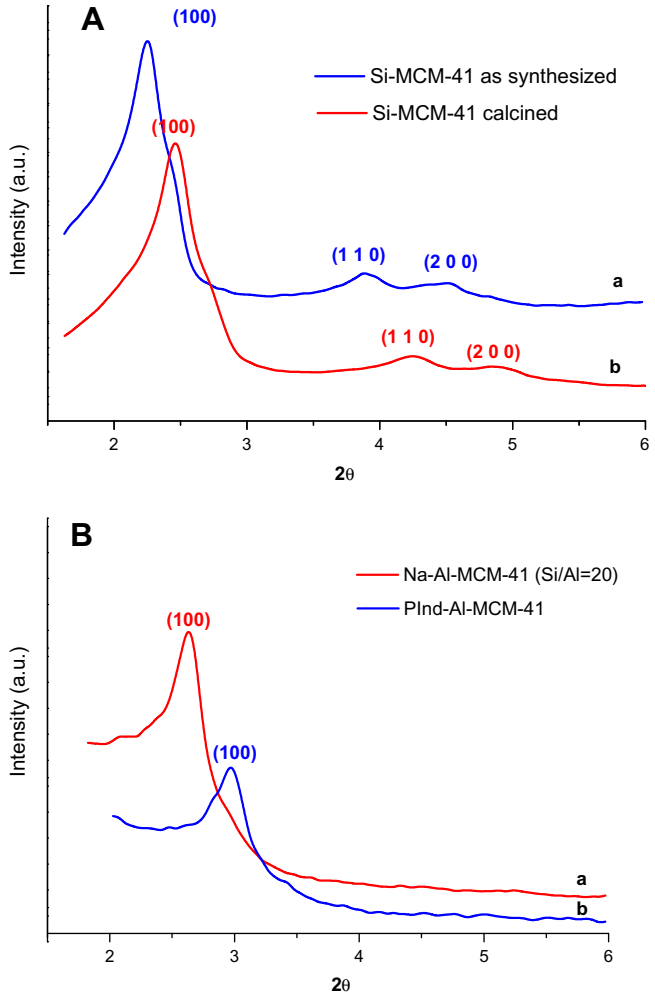

Fig. 5. X-ray diffraction patterns of (A) as synthesized and calcined Si-MCM-41 and (B) Na-AlMCM-41, and composite PInd–Na-AlMCM-41.

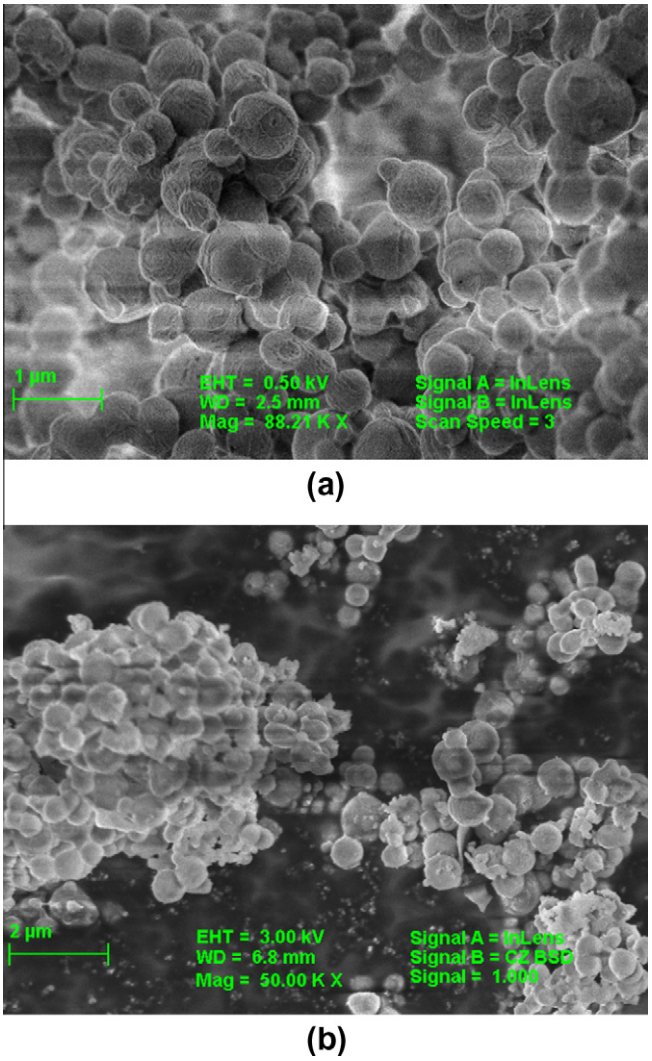

Fig. 6. SEM images of (A) Na-Al-MCM-41 and (B) PInd–Na-AlMCM-41 composite.

Table 2
Textural and structural properties of Si-MCM-41, Na-AlMCM-41 and PInd–Na-AlMCM-41.

Sample	*hkl*			a_o (nm)	Area m^2/g
	100	110	200		
	d (nm)				
Si-MCM-41*	39.11	22.63	19.52	4.5	–
Si-MCM-41**	35.62	20.72	18.04	4.1	1235
Al-MCM-41	33.70	19.50	—	3.8	860
PInd–Na-AlMCM-41	30.60	—	—	3.5	332

* As synthesized.
** Calcined.

The shift in the diffraction plane indicate that the two components (polymer and host) have been successfully integrated and the structure of composite is more orderly and uniform than that in pure Pind [21].

While the composite area is significantly smaller than that for the Na-AlMCM-41 host, its characteristic structure is maintained after the PInd nanowire is within the host, in agreement with the XRD studies (Table 2).

Fig. 6 shows SEM images of the (a) host and (b) composite. To establish the morphology of the materials, the SEM studies reveal that the incorporation of Pind by in situ polymerization were carried out in the pores of Na-AlMCM-41, having no apparent effects on the macroscopic morphology of the samples, and in which isolated clusters of Pind on the external surface of the composite are not observed. The SEM images of the samples show aggregates of regular spherulitic-shaped particles. The particle size on both samples was approximately 300–800 nm (550 nm average) in diameter.

3.3. UV–Vis studies of Polyindole and PInd–Al-MCM-41

Fig. 7 shows the UV–Vis spectra. Indole, polyindole and indole present in PInd–Al-MCM-41 composite were dissolved with dimethyl sulfoxide. Indole monomer has a single peak at 278 nm and polyindole has four peaks at 274, 307, 347 and 398 nm. The PInd–Al-MCM-41 composite shows the same spectrum as that of the polymer, with the same characteristic peaks.

In the literature, the UV–Vis spectrum of poly(5-methylindole) [22] shows a much broader absorption at 262, 310, 342 and 358 nm. And the absorption peaks of poly(5-cyanoindole) [23] are observed at 276, 319, 404 and 445 nm. The UV–Vis spectra of polyindole and its composite are very similar to those of its derivatives. Generally, the red shift of the absorption spectrum shows the increase in conjugated chain length [18].

Therefore, the UV–Vis spectra prove that it is possible to obtain in situ polymerization of indole, creating a new nano-composite, PInd–Al-MCM-41.

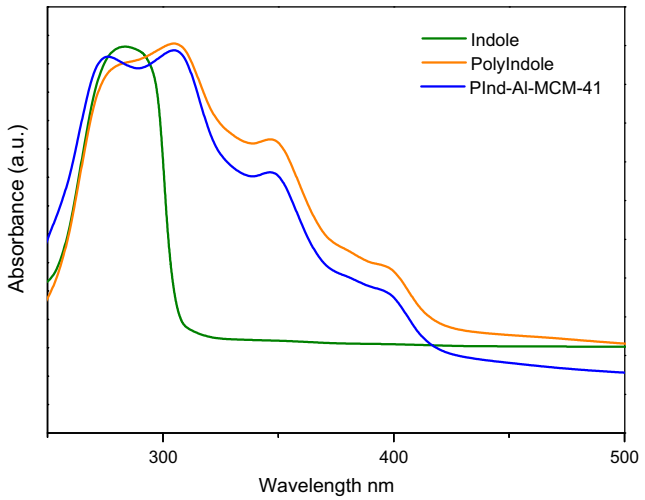

Fig. 7. UV–Vis spectra of indole, Polyindole and PInd–Al-MCM-41.

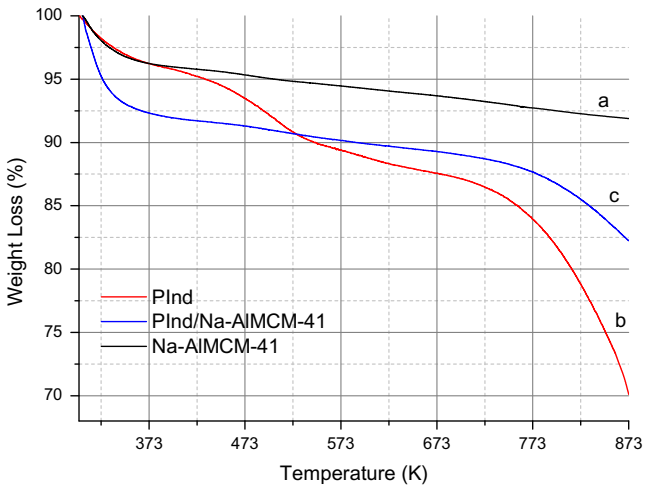

Fig. 8. TGA analysis for: (A) Na-AlMCM-41; (B) Pure polyindole; (C) PInd–AlMCM-41.

3.4. Thermal analysis

Fig. 8 shows the TGA curve analysis for Na-AlMCM-41 (a), Polyindole (b), and PInd–AlMCM-41 composite (c). For pure PInd (curve b), the initial weight loss (300–373 K) is caused by the loss of water from the polymer. The polymer is thermally stable up to 430 K. From this temperature, the polymer starts to degrade slowly; but above 700 K, the polymer degrades rapidly. For the Na-AlMCM-41 used as a host (curve a), the weight loss is about 4% around 373 K and then stabilizes with a total weight loss of 8.3% w/w when reaching 873 K. The composite (curve b) initial weight loss below 373 K can be attributed to the loss of water and to some gases adsorbed from the composite. It remains therefore fairly stable up to around 770 K. Above this temperature, the composite (the polymer mainly) starts to lose mass faster. If we considered the weight loss of pure PInd and guest PInd in the composite at 773 K, the difference would be wider (16% and 12.3%, respectively) but at 873 K this difference would be broader (17.8% and 30%, respectively). In consequence, PInd becomes more stable as a guest in the host forming the composite, preventing the polymer from a fast degrading. The total weight loss for the host and the composite is about 8.3% and 17.8% respectively at 873 K; the weight loss attributed to PInd in the composite (as a nano-guest) is about 10% w/w at 873 K. It should be noted that the total weight loss for pure PInd is near 30%.

3.5. Conductivity studies of PInd–AlMCM-41 nano-composite

According to literature data the electrical conductivity for chemically and electrochemically synthesized polyindole are 1×10^{-4} and 5×10^{-2} S cm^{-1}, respectively [18].

The PInd–Na-AlMCM-41 powder composite sample was pressed into pellets of 6 mm diameter and 0.7 mm thickness in a press by maintaining 2 ton metric pressure. These pellets were subjected to conductivity measurements in a four - probe set-up, improving the contacts with a silver layer. Resistances were determined from the current–voltage behavior and were converted into conductivity data using the dimensions of the pellet. The electrical conductivity of PInd–Na-AlMCM-41 nanocomposite at room temperature was in the range of 4×10^{-3} S cm^{-1}.

When conducting polymers are inside the pores of meso or microporous aluminosilicates (SBA, MCM, zeolites, etc.), the conductivity of the composite can change from insulating to ionic conductors through semiconductors [15]. The mechanism of conduction in conducting polymers, e.g., polyfuran, polyindole, polypyrrole and polyaniline, is highly complex, since such materials exhibit conductivity in a range of about ten orders of magnitude by changing their doping. To explain the electronic phenomena in these systems, the concepts of solitons, polarons and bipolarons have been used [24]. The conduction in conducting polymers (enhancing or dipping) is influenced by numerous factors: polaron length, conjugation length, overall chain length, and charge transfer to adjacent molecules [25]. Polyindole conductivity can change using different substituent. Conjugation length and redox potential are affected by their nature and substituent positions [26] and molecular orientation in conducting polymers clearly is a desirable characteristic, improving both inter and intra chain transport [27]. When the polymer is encapsulated in the host channels, conductivity may change. The mesoporous nanomaterial (MCM), used as a host, affects the movement of the charges in the polymer.

The composite has an electrical conductivity higher than that of the pure polymer synthesized by chemical method, approaching to pure polymer electrochemically synthesized. This behavior can be attributed to the fact that the Na-AlMCM-41 host increases the movement of the electrical charges through polyindole backbone content in the mesopores. Polyindole is possibly doped by the host.

4. Conclusions

Sodium aluminosilicate Na-AlMCM-41 material with longitudinal channel array was synthesized and characterized. The materials were analyzed by different methods (XRD, BET, SEM, UV–Vis and FTIR).

FTIR studies were carried out in order to analyze the nature of the interaction of indole adsorbed onto the mesoscopic material. Through infrared spectroscopy, we could observe that indole is adsorbed onto Na-AlMCM-41 in a large proportion through the π electron system with electron-acceptor sites of this material, like Na^+ cation and SiOH groups. The spectrum also shows that it is possible to obtain indole in situ polymerization within the Na-AlMCM-41 with hexagonal pore system. The composite obtained after in situ oxidative polymerization was analyzed by infrared spectroscopy and UV–Vis of Pind/host to corroborate the presence of polyindole. The bands that characterize this conductive polymer are present in the spectra.

The composites obtained were analyzed by X-ray diffraction, showing that after polymerization the porous structures of the materials are preserved and the PInd is found within the porous channels. The polymer is not on the surface but within the porous

channels, as indicated by BET, TGA and SEM. These composites offer numerous desirable properties potentially applied in the electronic field for developing, for instance, an electronic device at a nanometric scale. The composite has an electrical conductivity higher than the pure polymer chemically synthesized close to the electrical conductivity of pure polymer electrochemically synthesized. This behavior could be ascribed to the fact that Na-AlMCM-41 host increases the movement of the electrical charges through polyindole backbone content in the mesopores. Polyindole is possibly doped by the host.

Organic molecular wires have thus been successfully developed, together with an inorganic Na-AlMCM-41 reservoir (hybrid composite) into the channels.

Acknowledgments

MBGC, OAA and JC, CONICET Researchers, MLM CONICET postdoctoral fellowship and JMJ doctoral fellowship, are grateful to CONICET, Argentina, PIP N° 112-200801-00388 (2009-2012) and SCyT-CBA PID: 1210/07- (2007-2012).

References

[1] R. Schmidt, M. Stöcker, E.W. Hansen, D. Akporiaye, O.H. Ellestad, Micropor. Mater. 3 (1995) 443.
[2] C.T. Kresge, M.E. Leonowicz, W.J. Roth, J.C. Vartuli, J.S. Beck, Nature 359 (1992) 710.
[3] J.S. Beck, J.C. Vartuli, W.J. Roth, M.E. Leonowicz, C.T. Kresge, K.D. Schmitt, C.T.W. Chu, D.H. Olson, E.W. Sheppard, S.B. McCullen, J.B. Higgins, J.L. Schlenker, J. Am. Chem. Soc. 114 (1992) 10834.
[4] Z. Cai, G. Yang, Synthetic Met. 160 (2010) 1902–1905.
[5] D. Billaud, E.B. Maarouf, E. Hannecart, Polymer 35 (9) (1994) 2010–2011.
[6] P.S. Abthagir, R. Saraswathi, Thermochim. Acta 424 (2004) 25–35.
[7] P.C. Pandey, Sensor. Actuat. B-Chem. 54 (1999) 210–214.
[8] Z. Cai, C. Hou, J. Power Sources, in Press, Available online 22 August 2011.
[9] K.J. Mispa, P. Subramaniam, R. Murugesan, Int. J. Nanotech. Appl. 4 (2010) 147–152.
[10] L. Joshi, R. Prakash, Mater. Lett. 65 (2011) 3016–3019.
[11] D. Kumar, K. Schumacher, C. du Fresne von Hohenesche, M. Grün, K.K. Unger, Colloid. Surface. A 187–188 (2001) 109–116.
[12] O.A. Anunziata, A.R. Beltramone, J. Cussa, Catal. Today 133–135 (2008) 891–896.
[13] O.A. Anunziata, M.L. Martínez, M.B. Gómez Costa, Mater. Lett. 64 (2010) 545–548.
[14] M.L. Martínez, M.B. Gómez Costa, G.A. Monti, O.A. Anunziata, Micropor. Mesopor. Mater. 144 (2011) 183–190.
[15] M.L. Martínez, F.A. Luna D'Amicis, A.R. Beltramone, M.B. Gómez Costa, O.A. Anunziata, Mater. Res. Bull. 46 (2011) 1011–1021.
[16] O.A. Anunziata, M.B. Gómez Costa, M.L. Martínez, Catal. Today 133–135 (2008) 897–905.
[17] O.A. Anunziata, M.B. Gómez Costa, R.D. Sánchez, J. Colloid. Interf. Sci. 292 (2005) 509–516.
[18] H. Talbi, J. Ghanbaja, D. Billaud, Polymer 38 (1997) 2099–2106.
[19] S. An, T. Abdiryim, Y. Ding, I. Nurulla, Mater. Lett. 62 (2008) 935–938.
[20] V. Meynen, P. Cool, E.F. Vansant, Micropor. Mesopor. Mater. 125 (2009) 170–223.
[21] X. Sun, J. Ren, L. Zhang, L. Chen, H. Li, R. Li, J. Ma, Synthetic Met. 160 (2010) 2244–2249.
[22] J. Xu, J. Hou, S. Zhang, R. Zhang, G. Nie, S. Pu, Eur. Polym. J. 42 (2006) 1384–1395.
[23] J. Xu, W. Zhou, J. Hou, S. Pu, L. Yan, J. Wang, Mater. Chem. Phys. 99 (2006) 341–349.
[24] A.J. Heeger, in: T.A. Skotheim (Ed.), Handbook of Conducting Polymers, vol. II, Dekker, New York, 1986, p. 729. and references therein.
[25] J.I. Kroschwitz, in: J.I. Kroschwitz (Ed.), Electrical and Electronic Properties of Polymers: A State-of-the-Art Compendium, Wiley, New York, 1988, pp. 1–330.
[26] M. Leclerc, G. D'Aprano, G. Zotti, Synthetic Met. 55–57 (1993) 1527.
[27] C.D. Minto, A.S. Vaughan, Polymer 38 (1997) 2683–2688.